The Roles of Pore Ring and Plug in the SecY Protein-conducting Channel

James Gumbart and Klaus Schulten

Department of Physics and Beckman Institute, University of Illinois at Urbana-Champaign, Urbana, IL 61801

The protein-conducting channel, or translocon, is an evolutionarily conserved complex that allows nascent proteins to cross a cellular membrane or integrate into it. The crystal structure of an archaeal translocon, the SecY complex, revealed that two elements contribute to sealing the channel: a small "plug" domain blocking the periplasmic region of the channel, and a pore ring composed of six hydrophobic residues acting as a constriction point at the channel's center. To determine the independent functions of these two elements, we have performed molecular dynamics simulations of the native channel as well as of two recently structurally resolved mutants in which portions of their plugs were deleted. We find that in the mutants, the instability in the plug region leads to a concomitant increase in flexibility of the pore ring. The instability is quantified by the rate of water permeation in each system as well as by the force required for oligopeptide translocation. Through a novel simulation in which the interactions between the plug and water were independently controlled, we find that the role of the plug in stabilizing the pore ring is significantly more important than its role as a purely steric barrier.

The Journal of General Physiology

INTRODUCTION

Transport across membranes is a ubiquitous feature of living cells, typically requiring substrate-specific membrane-bound proteins that permit efficient passage for some molecules while preventing other molecules from breaching the membrane barrier. Proteins themselves are not excluded as substrates and often need to cross the membrane of the endoplasmic reticulum in eukaryotes or the plasma membrane in bacteria during or immediately after their formation while still in an unfolded state. One of the most common pathways involves the use of the protein-conducting channel, also known as the Sec61 or SecY complex (Veenendaal et al., 2004; Osborne et al., 2005; Pohlschröder et al., 2005; Wickner and Schekman, 2005; Rapoport, 2007). This channel works in concert with the ribosome or other channel partners, such as SecA in bacteria, which drive translocation of the nascent protein. The protein-conducting channel also serves as the point of insertion for most membrane proteins, thus requiring it to have two different modes of opening (van den Berg et al., 2004; Rapoport et al., 2004; White and von Heijne, 2005).

When not allowing the passage of proteins, the channel must maintain membrane integrity and prevent ions, protons, or other solutes from crossing; during protein translocation, the channel should also minimize the flow of other molecules. The crystal structure of an archaeal SecYEβ complex suggests a means by which the barrier could be maintained through the action of two structural elements in SecY, a pore ring and a plug, both shown in Fig. 1 (van den Berg et al., 2004). The plug, a small helix between transmembrane (TM) helices 1 and 2, blocks the periplasmic half of the hourglass-shaped channel, and the pore ring, composed of six hydrophobic residues, forms a constriction point at the channel's center. Multiple molecular dynamics (MD) simulation studies have shown the SecY complex to be watertight in its closed form, supporting the assertion that the pore ring and plug serve to close the channel (Gumbart and Schulten, 2006; Haider et al., 2006). Additionally, simulations of translocation revealed that the plug comes out of the channel, as expected, and the pore ring, known to contact the nascent polypeptide, forms a gasket-like seal around it (Cannon et al., 2005; Gumbart and Schulten, 2006; Bol et al., 2007). This seal is not expected to be perfect, but should still serve to maintain the permeability barrier (Schiebel and Wickner, 1992; Erlandson et al., 2008). An alternative model for sealing the channel has also been put forth based on fluorescence-quenching experiments in the eukaryotic system. In this model, it is proposed that the pore is quite large (up to 40–60 Å wide during translocation), and that it is sealed by the ribosome on the cytoplasmic side or by BiP on the luminal side (Crowley et al., 1994; Hamman et al., 1997, 1998). Whether or not this model applies in the prokaryotic system is unclear as there is no bacterial

Correspondence to Klaus Schulten: kschulte@ks.uiuc.edu

Abbreviations used in this paper: CA, constant area; CP, constant pressure; MD, molecular dynamics; RMSD, root mean-square deviation; RMSF, root mean-square fluctuation; SMD, steered MD; TM, transmembrane.

The online version of this article contains supplemental material.

The Rockefeller University Press $30.00
J. Gen. Physiol. Vol. 132 No. 6 709–719
www.jgp.org/cgi/doi/10.1085/jgp.200810062

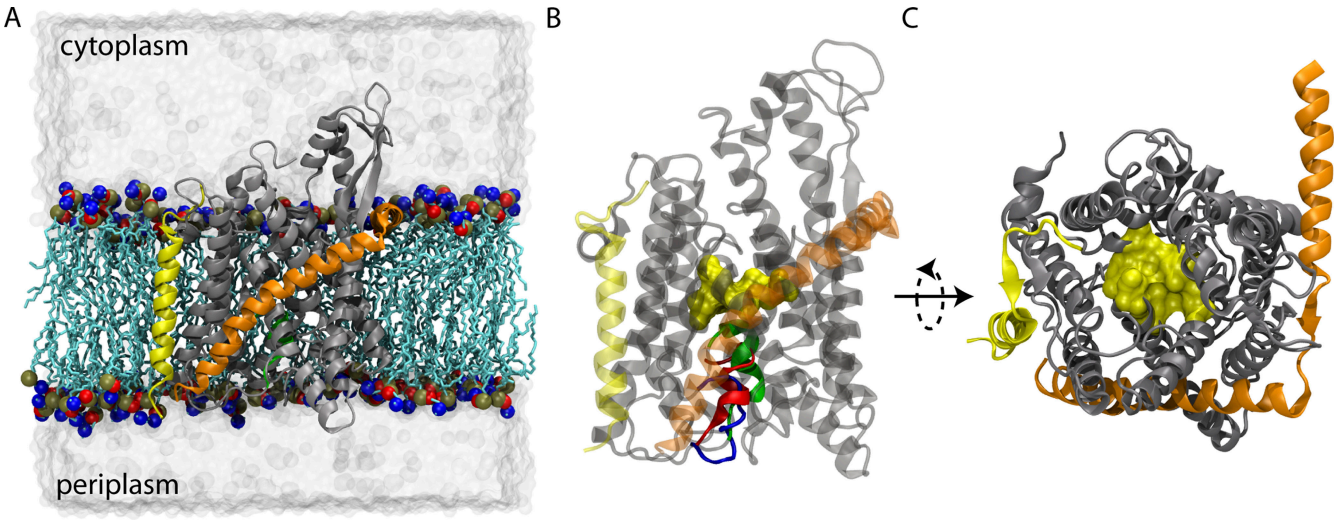

Figure 1. SecYEβ. In all panels, SecY is shown in gray, SecE in orange, and Secβ in yellow. (A) Side view of the simulated system. Lipids are colored light blue, with their head groups highlighted as red, blue, and brown spheres. Water is shown as a transparent, gray surface. (B) Comparison of SecYEβ crystal structures. The protein is transparent, with the pore ring drawn as a yellow space-filling surface in the center. The three structures are nearly identical except for the plugs. The native plug is shown in green, the half-plug deletion mutant in blue, and the full-plug deletion mutant in red. (C) View of SecYEβ from the cytoplasmic side. The pore ring is closed in all structures.

analogue to BiP known (Rapoport, 2007). Additionally, the SecY and Sec61 complexes have notable sequence similarity, particularly in regions such as the pore ring, suggesting that the complex functions similarly in all organisms (van den Berg et al., 2004).

Assuming pore ring and plug are both necessary to seal the channel, it has been unclear until recently what their independent roles are. Further confusing the situation is the fact that in multiple experiments, in *Saccharomyces cerevisiae* and *Escherichia coli*, deleting the plug was not lethal to the cell and, in fact, did not even significantly impair the channel's function (Junne et al., 2006; Maillard et al., 2007; Li et al., 2007). However, electrophysiology experiments demonstrated that deleting the plug makes the channel permeable to ions and causes it to alternate between open and closed states (Saparov et al., 2007). Crystal structures of two such plug deletion mutants were obtained, one a half-plug deletion mutant (residues 60–65 deleted) and one a full-plug deletion mutant (residues 57–67 deleted). Surprisingly, the structures showed that new plugs form from the remaining residues, and that the channel is still in a closed state (Li et al., 2007). We have examined through 0.35 μs of MD simulations the stability of these two mutants compared with the native channel. We find that the mutant channels permit the permeation of water due in part to increased fluctuations of the pore ring, whereas the native channel is watertight. We also observe that the force required for simulated translocation and for opening of the lateral gate, the site of membrane protein insertion, is reduced in the mutants, thus connecting plug deletion directly with channel function. Finally, through a unique simulation in which we uncouple the steric effects of the plug from its interactions with the rest of the channel, we are able to elucidate the specific roles of plug and pore ring. We conclude that the plug serves primarily to lock the channel in a closed conformation and that the pore ring is the primary barrier to the flow of water or ions through the channel, its widening and narrowing controlled through the plug.

MATERIALS AND METHODS

System Preparation

In total, four systems were built using the program VMD (Humphrey et al., 1996). Modeling of three of the systems, the native SecYEβ, the half-plug deletion mutant, and the full-plug deletion mutant, began from crystallographic structures (PDB codes 1RHZ, 2YXQ, and 2YXR, respectively; van den Berg et al., 2004; Li et al., 2007). The fourth system, a mutant with the plug locked outside of the channel, was prepared from the native structure by mutating residues 61 of SecY and 64 of SecE to cysteine using steered MD (SMD; see below) to pull the plug from the center of the channel, and then introducing a disulfide bond between the two residues. Each protein was placed in a POPC lipid bilayer solvated in water with 100 mM Na^+ and Cl^- ions neutralizing the system. The total size for all systems was ∼100,000 atoms. Additional details can be found in Gumbart and Schulten (2006).

MD Methods

Molecular simulations were performed using NAMD 2.6 (Phillips et al., 2005) and the CHARMM27 force field with the CMAP correction (MacKerell et al., 1998, 2004). Electrostatics were evaluated using a multiple time-stepping algorithm in which bonded interactions are calculated every 1 fs, short range non-bonded interactions every 2 fs, and long-range interactions every 4 fs. Long-range interactions were calculated with the particle mesh Ewald technique with a grid point density of $\sim 1/\text{Å}^3$.

All simulations were performed at constant temperature and pressure in the NpT ensemble. A constant temperature of 310 K was maintained using Langevin dynamics, applied to all heavy atoms with a damping constant of 1 ps^{-1}; in the case of SMD simulations, the thermostat was coupled only to the lipid heavy atoms to avoid affecting the measured force. A constant pressure (CP) of 1 atm was enforced via a Nosé-Hoover-Langevin piston. Additionally, for some simulations (denoted constant area [CA]), the area in the plane of the membrane was held constant while the *z*-dimension only was allowed to fluctuate to maintain a pressure of 1 atm. For all simulations, periodic boundary conditions were assumed.

Application of External Forces

SMD (Izrailev et al., 1997; Sotomayor and Schulten, 2007) was used for three sets of simulations. In the first set, deca-alanine, a 10-alanine helix, was pulled across the channel at 5 Å/ns, as done previously (Gumbart and Schulten, 2006); in the second set, the lateral gate was opened at 3 Å/ns, also as done previously (Gumbart and Schulten, 2007). In the third set, the plug was pulled away from the center of the channel at 1 Å/ns. Here, the plug was defined as residues 57–62 for the native SecYEβ, 54–59 for the half-plug deletion mutant, and 55–70 for the full-plug deletion mutant. In all cases, force was applied to the relevant atoms of the protein (C_α only) via a spring connected to an imaginary point moving at constant velocity. The force constant for this spring was 350 pN/$Å^2$ for translocating deca-alanine and for pulling the plug; for opening the lateral gate, a force constant of 175 pN/$Å^2$ was used.

To increase the pore opening in SecY for three simulations, a linear force pointing away from the center was applied only to protein atoms found within an imaginary cylinder of radius *r* centered on the pore ring. The radius was increased from 0 to 3.5 and then 5 Å at a rate of 1 Å/ns, after which the radius was maintained at each size (3.5 or 5 Å) for an additional 20 ns (see Table I).

Modification of Plug Interactions

To separately quantify the effect of plug and pore ring in maintaining the channel seal, a simulation modifying the interactions of the plug with water was performed for the closed native state of the channel. The plug (residues 55–65) maintained normal bonded and non-bonded interactions with the rest of the protein, lipids, and ions. However, non-bonded interactions between plug and water (van der Waals and short-range electrostatic interactions) were turned off, effectively making the two "transparent" to each other. This was accomplished by developing a modified version of NAMD in which the interactions could be controlled separately. The source code for this version is available upon request.

Analysis

Osmotic Permeability. We calculated the osmotic permeability, p_f, from equilibrium simulations following the procedure developed in Zhu et al. (2004a) and also validated elsewhere (Aksimentiev and Schulten, 2005; Hashido et al., 2005; Jensen and Mouritsen, 2006). In brief, a collective coordinate describing the motion of all water molecules in the channel is defined via the relation

$$dn = \sum_{i \in S(t)} dz_i / L, \tag{1}$$

where $S(t)$ is the set of water molecules in the channel at time t, dz_i is the movement of water molecule i in the z-direction at time t, and L is the length of the channel (defined for SecY as 40 Å). By setting $n(0) = 0$, Eq. 1 can be integrated to give $n(t)$. We divided $n(t)$ into M 2-ns subtrajectories, setting each $n_i(0) = 0$. The mean square displacement (MSD) was then calculated using

$$\mathrm{MSD}(t_j) = \frac{1}{M}\sum_{i=1}^{M} n_i(t_j)^2, \tag{2}$$

with t_j ranging from 1 to 100 ps, in 1-ps increments. At equilibrium, $n(t)$ follows a 1D random walk, and thus $\langle n^2(t)\rangle = 2D_n t$. A linear regression was used to fit $\mathrm{MSD}(t_j)$ versus t_j, giving the diffusion coefficient D_n. Finally, p_f is connected to D_n through the relationship

$$p_f = \nu_W D_n, \tag{3}$$

where ν_W is the average volume of a single water molecule (18 cm^3/mol; Zhu et al., 2004a). Standard deviation was determined by comparing multiple values of p_f calculated for each subtrajectory.

TABLE I

Water Permeation through SecY

System	Time(ns)	CP/CA	Wat. Up	Wat. Down	Rate (/ns)	p_d (10^{-13} cm^3/s)	p_f (10^{-13} cm^3/s)
native	20.0	CP	0	0	0	0	0
native	10.0	CA	0	0	0	0	0
Δ57–67	51.0	CP	203	220	8.29 ± 4.00	1.24 ± 0.60	5.34 ± 1.85
Δ57–67 (first 20 ns)	20.0	CP	46	64	5.50 ± 1.32	0.82 ± 0.20	5.03 ± 1.84
Δ57–67	20.0	CA	46	65	5.55 ± 2.74	0.83 ± 0.41	4.31 ± 1.43
Δ57–67 (rest.)	20.0	CP	0	0	0	0	0
Δ60–65	20.0	CP	14	6	1.00 ± 1.19	0.15 ± 0.18	2.92 ± 0.77
Δ60–65	20.0	CA	2	2	<1	N/A	N/A
plug-SecE–locked	20.0	CP	24	12	1.80 ± 1.91	0.27 ± 0.29	3.95 ± 2.01
plug-SecE–locked	20.0	CA	12	13	1.25 ± 1.48	0.19 ± 0.22	3.51 ± 1.60
r_{pore} = 3.5 Å	20.0	CP	230	196	21.30 ± 2.13	3.18 ± 0.32	9.50 ± 4.20
r_{pore} = 3.5 Å (rest.)	20.0	CP	195	148	17.15 ± 3.79	2.56 ± 0.57	9.29 ± 3.32
r_{pore} = 5 Å	20.0	CP	759	643	70.10 ± 8.63	10.48 ± 1.29	25.96 ± 7.96
transp. plug	20.0	CP	1	5	<1	N/A	N/A

Simulations are listed by system, time, and pressure conditions. "Transp. plug" denotes the simulation in which the plug was made transparent to water. "Rest." indicates the simulations where the pore ring residues were restrained to their initial positions. "CP" means constant pressure was maintained in all dimensions, and "CA" means constant area in the plane of the membrane was enforced. The number of water permeation events up (from periplasmic to cytoplasmic) and down (cytoplasmic to periplasmic) through the channel is given, along with the bidirectional permeation rate, the diffusive permeability (p_d), and osmotic permeability (p_f). For simulations in which the number of permeation events was <1/ns, permeabilities were not calculated.

Diffusive Permeability. The diffusive permeability, p_d, was calculated using

$$p_d = \nu_W q_0, \quad (4)$$

where q_0 is the unidirectional number of permeation events per unit time (i.e., half the rate reported in Table I; Zhu et al., 2004b). Standard deviation for p_d as well as the permeation rate were found by dividing the full trajectory into 5-ns subtrajectories and calculating p_d and the rate for each.

Online Supplemental Material

The online supplemental material contains additional analyses and figures. The membrane area as a function of time is presented in Fig. S1. Also, the water density inside the pore and distribution of water occupancies for the full-plug deletion mutant as well as the two simulations of the plug-SecE–locked mutant with r_{pore} = 3.5 Å are presented and discussed in more detail (Figs. S2 and S3). The pore radius as a function of time is given for all systems in Figs. S4 and S5. Fig. S6 compares the size of a water molecule to that of the closed pore ring. Figs. S7 and S8 illustrate the fluctuations of the pore ring residues and the plug over time, respectively. Fig. S9 compares the pore rings in the three crystal structures, whereas Fig. S10 compares the intrusion of water into the pore during the simulations. Finally, Fig. S11 compares the force required for lateral gate opening to that measured in a previous study (Gumbart and Schulten, 2007). The online supplemental material is available at http://www.jgp.org/cgi/content/full/jgp.200810062/DC1.

RESULTS

To discern the dynamic differences between native SecY and its two plug deletion mutants, which appear quite similar structurally, we performed long equilibrium simulations of each. In addition to systems for the native SecY, the half-plug deletion mutant, and the full-plug deletion mutant, we also modeled SecY with the plug disulfide bonded to SecE outside of the channel (residues 61 in *Methanococcus jannaschii* SecY and 64 in SecE). This "plug-SecE–locked" mutant is known to be lethal and has the highest conductance of the channel mutants tested in experiment (Harris and Silhavy, 1999; Tam et al., 2005; Saparov et al., 2007). Each mutant was simulated for at least 20 ns in two separate simulations, one in which the membrane area was fixed (denoted CA) and one in which the pressure in all dimensions was held constant (denoted CP). Although a significant difference is not expected between CA and CP simulations, CP simulations with the CHARMM force field can produce overcompressed bilayers, which, in principle, could affect the behavior of the channel (Feller and Pastor, 1999; Gullingsrud and Schulten, 2004). Indeed, in our CP simulations, compression was weak as the area became reduced by only ~6% (see Fig. S1, available at http://www.jgp.org/cgi/content/full/jgp.200810062/DC1).

Permeability of the Resting Channel

As recent experiments indicated large differences in the conductance of each mutant, we first chose to quantify the permeability for all systems. No water or ion permeation was observed for native SecY (see Table I), as expected from previous simulations and from experiment (Gumbart and Schulten, 2006; Haider et al., 2006; Saparov et al., 2007). Ion conduction was not observed for the mutants either; therefore, we used water conduction as a surrogate measure of channel openness.

The theory and simulation of water permeation through channels are described in Zhu et al. (2004b), in particular the difference between the diffusive (p_d) and osmotic (p_f) water permeability as well as the rate of water molecules permeating the channel; the latter property is easy to obtain from simulation (see also Materials and methods) whereas p_d and, in particular, p_f are relatively easy to observe experimentally. A water permeation event was counted when a water molecule crossed the pore ring and moved at least 3 Å beyond it. As seen in Table I, the full-plug deletion mutant had the highest rate of water permeation at 5.5/ns (over the first 20 ns), followed by the plug-SecE–locked channel at 1.8/ns, and then the half-plug deletion mutant at 1.0/ns (all from the CP simulations). Although we would expect the plug-SecE–locked channel to have the highest conductance based on experiments (Saparov et al., 2007), the pore ring of the full-plug deletion mutant is more distorted due to the recruitment of additional residues to form the new plug. The plug-SecE–locked mutant may form over time a new plug from available residues, leading to similar distortions in the pore ring and conduction at an even higher rate. CA simulations (see Materials and methods) produced similar results, with the exception of the conduction of the half-plug deletion mutant being less. We also found that the rate of water permeation for the full-plug deletion mutant increases over 51 ns to an average value of 8.29/ns. This increase in the rate and its standard deviation suggest that over time, structural changes may cause the channel to become more permeable; the increase can also be seen by looking at cumulative permeation events, shown in Fig. S2, which is available at http://www.jgp.org/cgi/content/full/jgp.200810062/DC1.

To relate the present simulations to experimental observation, we calculated the osmotic permeability, p_f (see Materials and methods), from the equilibrium simulations. Resulting p_f values fall into the range 2–5 × 10^{-13} cm^3/s, comparing well to p_f measured for some aquaporins (e.g., aquaporins 1 and 4; Yang and Verkman, 1997; Pohl, 2004). The simulations as a whole indicate that although the mutants appear closed in the crystal structures, they actually fluctuate between closed and open states in their native environment, permitting water to permeate.

To determine the source of the increased permeability in the mutant channels, we first considered a role of the six pore ring residues. After the addition of hydrogen atoms (see Materials and methods), the opening formed

by the pore ring is smaller than the 5–8 Å originally seen in the crystal structures and can hardly accommodate a single water molecule at any given time (see Fig. S6, available at http://www.jgp.org/cgi/content/full/jgp.200810062/DC1; van den Berg et al., 2004). However, despite their similar initial appearance in all the structures, the pore rings in the mutants exhibit greater fluctuations compared with the native one. Fig. 2 B shows the root mean-square deviation (RMSD) of the pore ring residues over time. The pore rings of the half-plug and full-plug deletion mutants show larger deviations over time compared with the native pore ring, although much of the deviation comes from early distortion of the residues. Because RMSD measures the net movement of the residues, and thus is less sensitive to small fluctuations, we also measured the *z*-coordinate of the terminal heavy atom of each pore ring residue's side chain as a function of time. As shown in Fig. S7 (available at http://www.jgp.org/cgi/content/full/jgp.200810062/DC1), the residues of the half- and full-plug deletion mutants demonstrate much greater fluctuation and overall deviation compared with the native SecY. To confirm the relationship between fluctuation of the pore ring residues and conduction, we simulated the full-plug deletion mutant with the heavy atoms of the pore ring restrained to their initial positions. During 20 ns of simulation, we found that not a single water molecule crossed the restrained pore ring, indicating that the pore's small size in the crystal structure is sufficient to prevent permeation, the hydrophobic nature contributing possibly to this behavior. Although the pore ring does not adopt a permanently open conformation in unrestrained simulations, it does exhibit fluctuations that permit passage of water and presumably also of ions and other small molecules.

To determine how far pore hydrophobicity controls water permeation for large openings, we simulated the plug-SecE–locked mutant with enforced inner pore radii of 3.5 and 5 Å (see Materials and methods). Earlier simulations suggest that water conduits in hydrophobic nanopores become disrupted for pore radii decreasing below 4 Å, the actual transition depending on pore length among other factors (Beckstein et al., 2001). Our simulations showed that SecY at both pore radii remained primarily water-filled, i.e., open; at r_{pore} = 3.5 Å, 426 water permeation events were observed in 20 ns, and at r_{pore} = 5 Å, 1,402 permeation events were observed. The corresponding p_f is 2.6×10^{-12} cm^3/s for the wider pore, which compares well with the p_f value of nonselective channels like α-hemolysin (Paula et al., 1999; Pohl, 2004). The length of the hydrophobic region in SecY is shorter at 6 Å than the length investigated by Beckstein et al. (2001) (8–12 Å) as well as that in other channels, e.g., the mechanosensitive channel MscS (10 Å, comprised of two rings of hydrophobic residues) and the nicotinic acetylcholine receptor (14 Å, three rings of hydrophobic residues;

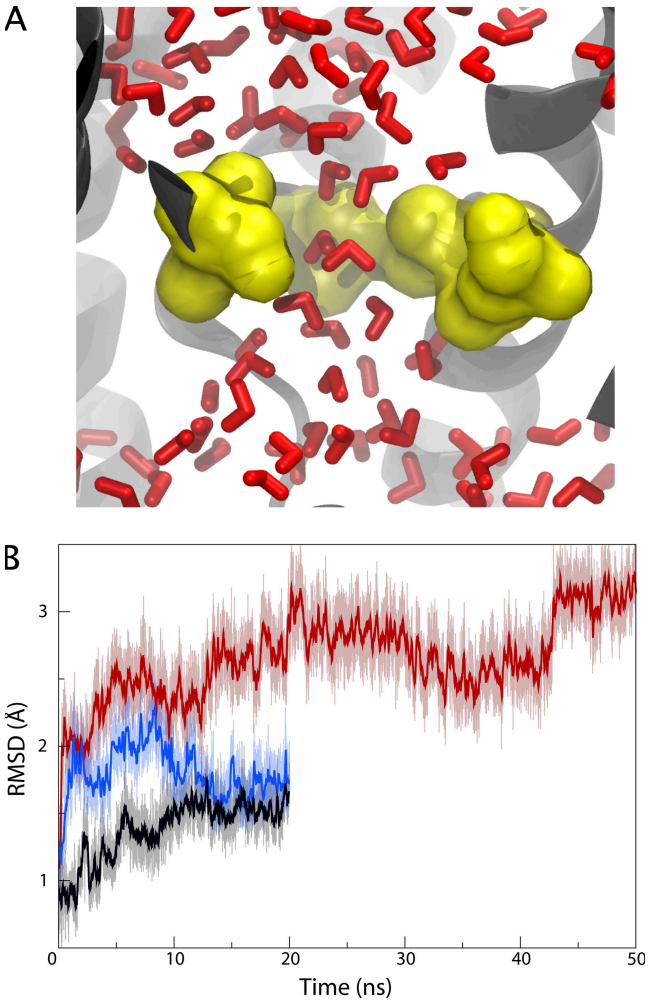

Figure 2. Effect of plug deletion on the pore ring. (A) Water permeation in the full-plug deletion mutant. A snapshot of the pore ring, in yellow, from the equilibrium simulation is shown. Pore ring residues Ile^{75} and Ile^{174} are not shown for clarity. Water molecules (red) flow easily through the pore ring, which is captured in an open state. (B) RMSD of the pore ring residues. The RMSD for the pore rings of native SecY (black), its half-plug deletion mutant (blue), and its full-plug deletion mutant (red) are shown as a function of time. Solid lines denote the running averages of the transparent ones.

Anishkin and Sukharev, 2004; Sotomayor and Schulten, 2004; Beckstein and Sansom, 2006). Apparently, SecY's pore ring is too short to block the flow of water at intermediate radii, but the decreased water density inside the pore ($n(t)/n_{bulk}$ = 0.6 on average; see Online supplemental material) may be sufficient to prevent the passage of ions (Beckstein and Sansom, 2003).

To investigate the role of pore ring residue fluctuations in water permeation, we simulated the plug-SecE–locked mutant at r_{pore} = 3.5 Å with its pore ring residues completely restrained. As seen in Table I, the rate of water permeation is decreased compared with the freely fluctuating pore ring. For the unrestrained pore ring, we found that a symmetric water distribution peaked at

n = 5–6 water molecules (see Online supplemental material); for the restrained pore ring, a bimodal distribution was found, peaked at n = 0 ("vapor-like" state) and at n = 5 ("liquid-like" state) inside the pore ring, indicative of hydrophobic gating (Beckstein and Sansom, 2006). Thus, pore ring residues' fluctuations impair hydrophobic gating effects.

One of the most surprising features of the mutant structures is that despite missing half or all of the original plug, new plugs formed from the remaining residues (Li et al., 2007). However, these plugs form fewer interactions with the rest of the channel than seen in the native case, and therefore do not remain in the center of the channel as in native SecY (see Fig. 1). In native SecY, the plug forms hydrophobic interactions with the pore ring as well as with TMs 2b and 7 that form the lateral gate. In the half-plug deletion mutant, hydrophobic residues in the new plug interact predominantly with the loops between TMs 3 and 4 and TMs 7 and 8. Interactions in the full-plug deletion mutant are even weaker, with the new plug interacting mostly with the N-terminal end of TM 2b and also with Gln^{180} in TM 5. The loss of many interactions permits the new plugs greater freedom to move within the channel. Although for the native SecY the plug's center of mass moves by only (0.7 ± 0.16) Å, the plugs for the half-plug deletion mutant and the full-plug deletion mutant move by as much as (2.7 ± 0.28) and (4.7 ± 0.33) Å from their starting positions, respectively, and both exhibit larger fluctuations over time (see Fig. S8, available at http://www.jgp.org/cgi/content/full/jgp.200810062/DC1). As the plug acts in part to block the periplasmic half of the channel, its additional movement in the mutants likely also facilitates the permeation of water as observed in our simulations.

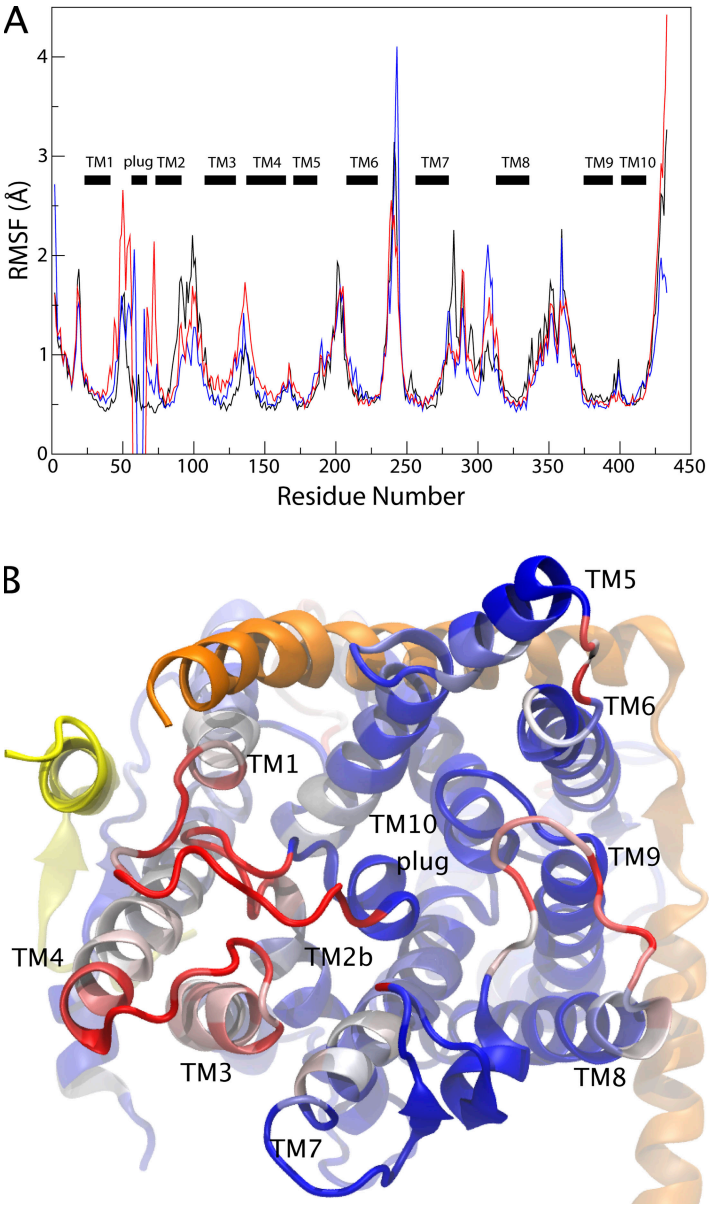

Figure 3. Effect of plug deletion on SecY. (A) RMSF of SecY. The RMSF calculated over the last 17.5 ns of a 20-ns trajectory is shown for native SecY (black) as well as its half-plug deletion mutant (blue) and its full-plug deletion mutant (red). The locations of the TM segments are indicated in the plot. (B) SecY viewed from the periplasmic side. SecY is colored according to the difference between the RMSF for the full-plug deletion mutant and native SecY, with red representing the largest difference and blue the smallest. SecE and Secβ are shown in orange and yellow, respectively.

In addition to affecting the pore ring, modifications of the plug affected other parts of the channel as well. We compared the root mean-square fluctuations (RMSFs) of all residues for each simulation, shown in Fig. 3 A. Fluctuations for residues of the native SecY are highest in the cytoplasmic loops, including channel-partner binding loops 6/7 and 7/8, in agreement with other simulations (Haider et al., 2006). For the mutants, residues with increased fluctuations compared with native SecY correspond primarily to those near the plug, including TM1 as well as the loops between TMs 3 and 4 and TMs 7 and 8, illustrated in Fig. 3 B. Although the pore itself did not widen significantly on the timescale of our simulations, the localized increase in fluctuations in the periplasmic half of the channel may over time lead to spontaneous widening. This additional widening outside of the timescale of our simulations may also account for the significant ion permeation measured in experiment but not observed in our simulations.

Forced Opening of the Channel

To further elucidate differences between the mutant structures, we performed three sets of SMD simulations (see Materials and methods). In the first two sets, we simulated translocation of a deca-alanine helix across the channel and also simulated forced lateral gate opening, following simulations performed previously (Gumbart and Schulten, 2006, 2007). In the third set, we applied force to the plug, pulling it out of the channel toward the periplasm. In all cases, the element of interest, deca-alanine, the lateral gate, or the plug, was pulled at a constant velocity while the force required was measured.

It has been suggested that *prl* mutations of the translocon, a class of known mutations that decrease or eliminate the need for a signal sequence to initiate translocation, function often by destabilizing the closed state of the channel (Smith et al., 2005). Similarly, mutations that bias SecY toward a more open state should presumably also more easily permit the passage of polypeptides. To examine the connection between mutations in the channel and translocation, we pulled deca-alanine across the native channel (toward the periplasm) as well as across the half-plug and full-plug deletion mutants (each simulation requiring 10 ns in total). The force for each system as a function of position along the channel axis is presented in Fig. 4 A. Although the forces are large due to the speed of the enforced translocation, they are comparable to those measured in other SMD simulations of SecY (Gumbart and Schulten, 2006; Sotomayor and Schulten, 2007). A clear trend can be recognized in the magnitude of force required for translocation. The force for the half-plug deletion mutant at its peak is ~10% less than that for the native channel, and for the full-plug deletion mutant it is ~35% lower. As in previous simulations, the peak in force for all systems corresponds to the expansion of the pore ring (Gumbart and Schulten, 2006),

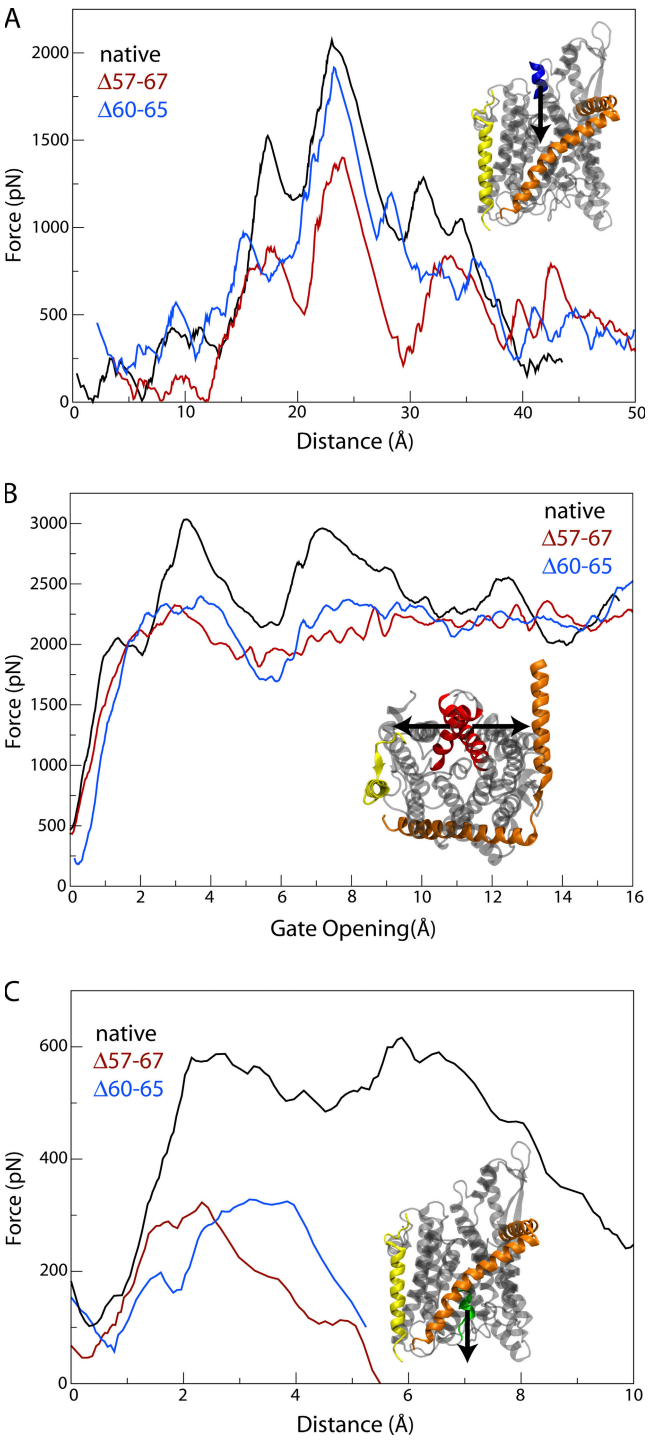

Figure 4. SMD of SecY. The colors in each plot are the same: black for native SecY, blue for the half-plug deletion mutant, and red for the full-plug deletion mutant. (A) Translocation across the channel. Shown is the force required as a function of position for translocation of deca-alanine (all values have an SD of 120 pN). (B) Opening of the lateral gate. The force required to open the lateral gate is shown as a function of the size of the gate opening (SD = 375 pN). (C) Plug removal. The force required to pull the plug out of the channel is shown as a function of distance pulled (SD = 120 pN).

indicating that the pore ring opens more easily in the mutants than in the native channel.

Further SMD simulations focused on opening the lateral gate of SecY, the point of insertion for membrane protein segments, formed between TMs 2b and 7 (van den Berg et al., 2004). We forced the gate open by pulling the C_α atoms of the gate helices for 6 ns in opposite directions. The measured forces, compared with those previously found for native SecY (Gumbart and Schulten, 2007), are shown in Fig. 4 B. The mutants require noticeably less force to open the gate, with as much as 33% less force required at an opening of 6–9 Å, the relevant range being the same as seen before (Gumbart and Schulten, 2007); after an opening of 9 Å, the forces become equivalent as the plug is then completely free in all systems.

To quantify the decreased interactions of the new plugs with the channel body, we pulled each plug out of the channel at 1 Å/ns, again measuring the force required, shown in Fig. 4 C. Because the plugs started at different positions within the pore for each channel, the force required at specific positions cannot be directly compared. Nonetheless, we see a clear difference between the native channel and the two mutants. The force required to remove the plugs for both mutants is half of that required for the native channel. The lower force needed for the mutants agrees well with the previous analysis indicating that the new plugs are not nearly as stable as the native plug in the channel's closed state. Thus, it is likely that the decreased stability of the plugs is a contributing factor to the decrease in force required for translocation in the two mutants, although by how much it alone lowered the force is unclear.

Modification of Plug Interactions

Given that the two elements, plug and pore ring, normally function in a cooperative manner, and that disturbing one affects the other (Gumbart and Schulten, 2006), determining their independent contributions to sealing the channel is difficult. To address this difficulty, we performed an additional simulation in which the plug was made "transparent" for water molecules. Specifically, for the native SecY, interactions (electrostatic and van der Waals) between plug residues 55–65 and water were turned off. All other interactions were maintained, including those between the plug and the rest of the channel. Water molecules could pass through the plug unperturbed, as illustrated in Fig. 5, but still permitted the plug to lock the channel in a closed conformation. By separating the two roles of the plug in a manner only possible in simulation, we can assess whether the pore ring, when interacting with the plug, is sufficient to block the channel.

As before, we counted permeation events over the course of the 20-ns simulation, and the results are shown in Table I. We found that only six water molecules crossed the pore ring, significantly less than in the case of the mutants; additionally, the plug was nearly as immobile as in the simulation with all interactions maintained (not depicted). We also monitored the z-coordinates of the pore ring side chains, shown in Fig. S7. The pore ring residues did not deviate significantly from their starting positions, with the exception of Ile^{260}. Fluctuations were also small compared with those for the mutants.

If the plug merely served as a steric barrier to the flow of water and ions, one would expect that the conductance measured in this simulation would be on par with or greater than that of the mutants. Given that the conductance is actually only ~15% of that for the plug-SecE–locked mutant, the plug's interactions with the rest of the channel must play an important role in sealing it. In particular, the plug holds the pore ring residues in place, which in turn maintain a nearly watertight seal. Thus, the pore ring is the primary barrier to the flow of water, whereas the plug serves to hold the pore ring and channel in a closed conformation.

DISCUSSION

The structure of the protein translocon revealed a channel tightly closed by two elements, the plug and the pore ring, although it remained unclear precisely how each contributes to sealing the channel. Crystal structures of plug deletion mutants showed the channel to be closed, due in part to the formation of new plugs from the remaining residues (Li et al., 2007). Although these structures suggest that the plug is a critical element of the channel, electrophysiology experiments showed that the new plugs apparently are not sufficient seals because the mutants alternated between open and closed states, permitting a significant flux of ions over long timescales (Saparov et al., 2007). Now with MD simulations, we have clarified the roles of both plug and pore ring in maintaining a closed channel. To determine why the mutants are more permeable than native SecY, we ran simulations on each of the three crystal structures of SecY (the native channel, the half-plug deletion mutant, and the full-plug deletion mutant) as well as a mutant modeled with the plug locked to SecE outside the channel. We also resorted to three sets of SMD simulations, including simulated translocation of a deca-alanine helix and lateral gate opening, to further quantify the distinction between the structures. Finally, a unique simulation in which the interactions between plug and water were turned off allowed us to definitively assess the relative importance of the roles of the plug as a steric barrier and as a lock restricting movement of the rest of the channel.

The equilibrium simulations revealed that although the native SecY is watertight, the plug deletion and plug-SecE–locked mutants permitted permeation of water. We also saw that the new plugs in the mutant structures are less stable than in native SecY. Previous simulations of translocation indirectly showed that the plug and the

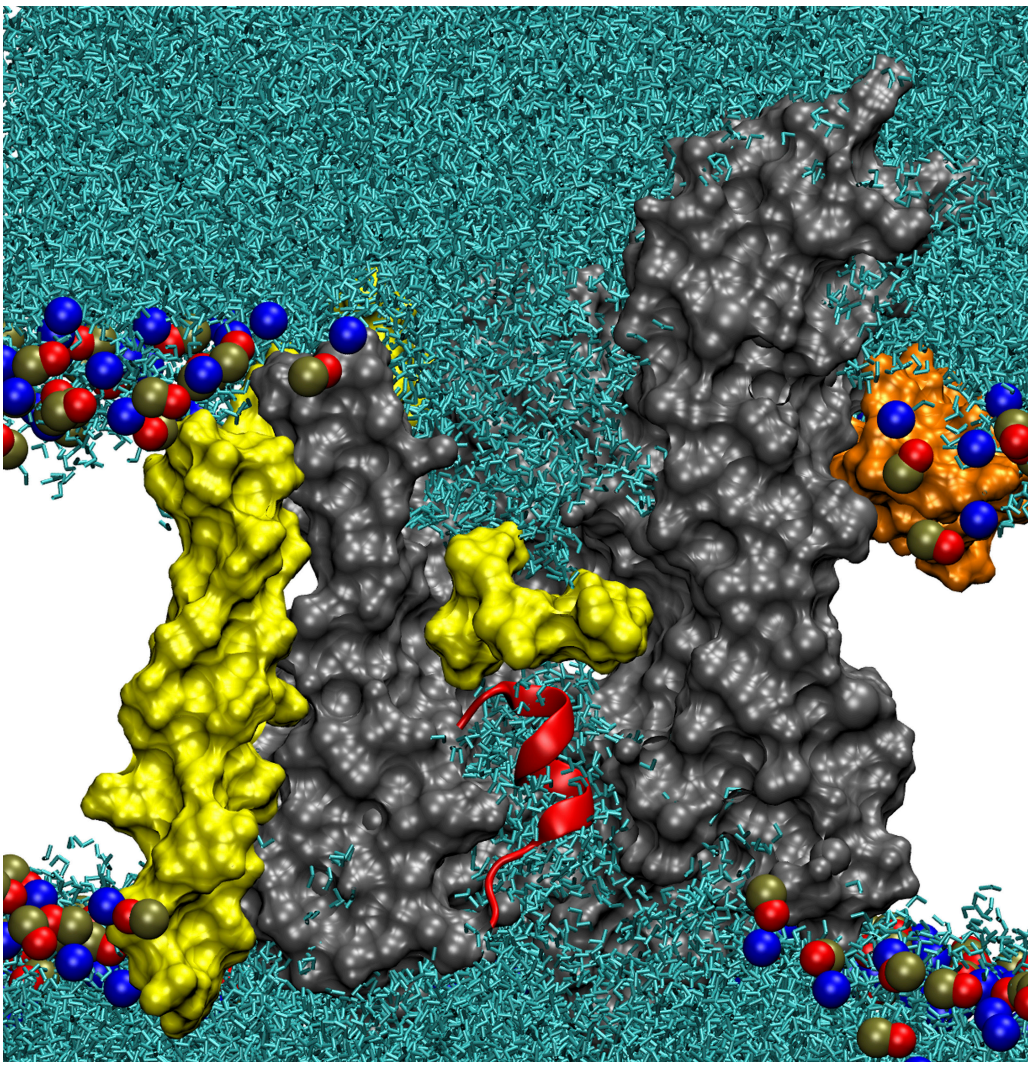

Figure 5. Modification of the plug's interactions with water. SecYEβ is shown as a molecular surface, colored as in Fig. 1, cut through the middle to display the channel. Lipid head groups are indicated as blue, red, and brown spheres. Water molecules, shown in light blue, fill the channel up to the pore ring, in yellow, from both top and bottom. The water molecules clearly overlap the plug, shown in red.

pore ring were not independent and that opening one apparently destabilized the other (Gumbart and Schulten, 2006). The current results confirm the connection between the two in opening the channel; the unstable plugs in the mutant structures permit the pore ring residues to move more freely, leading to the observed water permeation events. When the pore ring in the full-plug deletion mutant was restrained to its crystallographic radius, not a single water molecule crossed the channel; at larger pore ring radii, a vapor-like state in the pore was only observed when the pore ring was restrained. Both results further illustrate that the pore ring's dynamic behavior is responsible for the channel's permeability. SMD simulations also indicate that the mutant channels permit translocation and lateral gate opening more easily than the native, closed SecY, suggesting why deleting the plug negates the requirement of a signal sequence for channel opening (Li et al., 2007). The decreased force required for translocation is also in agreement with experiments that found a particular plug deletion mutant had a sixfold increase in translocation activity (Maillard et al., 2007). The connection between the plug and pore ring became most apparent when we simulated the native SecY with interactions between water and plug eliminated, permitting water to freely pass through the plug. Even after eliminating artificially the steric barrier presented by the plug, only a few water molecules crossed the pore ring, significantly fewer than in the mutants, illustrating that the plug's primary function is to lock the channel in a closed conformation.

Our results further illustrate the proposed steps in the gating of SecY (Smith et al., 2005; Li et al., 2007). When a signal sequence is inserted into the channel, it is known to be in contact with TMs 2b and 7 (the lateral gate) as well as lipids (Plath et al., 1998; Higy et al., 2005).

Whether the lateral gate fluctuates spontaneously to an open state or is opened through interaction with the signal sequence and then held in the open position is still unknown. However, once the gate is held open, its interactions with the plug are broken, loosening and even freeing the plug, as seen in previous simulations (Gumbart and Schulten, 2007). The present simulations demonstrate that once the plug is loosened, the pore ring fluctuates more and permits translocation more easily. Although we only observed periplasmic portions of the channel becoming destabilized in the plug deletion mutants, experiments suggest that over longer timescales, the destabilization would propagate to the rest of the channel (Junne et al., 2006; Saparov et al., 2007). Gating efficiency is also likely increased by the binding of channel partners and dimerization. Previous simulations showed that in a back-to-back dimer, the plugs are less stable compared with the monomer as also suggested by experiment (Bostina et al., 2005; Tam et al., 2005; Gumbart and Schulten, 2006). Binding of the translocon to the ribosome or SecA, required to initiate translocation, may increase the opening probability of the channel as well. For example, ribosome–channel complexes with the nascent chain removed are permeable to ions and small molecules, suggesting at least that the ribosome can prevent the channel from closing (Simon and Blobel, 1991; Heritage and Wonderlin, 2001). However, the full effect of the channel partners on SecY is still unknown; in particular, it is unknown whether channel partners affect the channel's opening, and to what degree.

The authors thank Shawn Brown at the Pittsburgh Supercomputing Center for assistance. All molecular images were made using VMD (Humphrey et al., 1996).

This work was supported by the National Institutes of Health (grants R01-GM067887 and P41-RR05969). The authors gratefully acknowledge computer time provided by the Pittsburgh Supercomputing Center and the National Center for Supercomputing Applications through the National Resources Allocation Committee (MCA93S028).

Lawrence G. Palmer served as editor.

Submitted: 11 June 2008
Accepted: 23 October 2008

REFERENCES

Aksimentiev, A., and K. Schulten. 2005. Imaging alpha-hemolysin with molecular dynamics: ionic conductance, osmotic permeability and the electrostatic potential map. *Biophys. J.* 88:3745–3761.

Anishkin, A., and S. Sukharev. 2004. Water dynamics and dewetting transitions in the small mechanosensitive channel MscS. *Biophys. J.* 86:2883–2895.

Beckstein, O., and M.S.P. Sansom. 2003. Liquid-vapor oscillations of water in hydrophobic nanopores. *Proc. Natl. Acad. Sci. USA.* 100:7063–7068.

Beckstein, O., and M.S.P. Sansom. 2006. A hydrophobic gate in an ion channel: the closed state of the nicotinic acetylcholine receptor. *Phys. Biol.* 3:147–159.

Beckstein, O., P.C. Biggin, and M.S.P. Sansom. 2001. A hydrophobic gating mechanism for nanopores. *J. Phys. Chem. B.* 105:12902–12905.

Bol, R., J.G. de Wit, and A.J.M. Driessen. 2007. The active protein-conducting channel of *Escherichia coli* contains an apolar patch. *J. Biol. Chem.* 282:29785–29793.

Bostina, M., B. Mohsin, W. Kühlbrandt, and I. Collinson. 2005. Atomic model of the *E. coli* membrane-bound protein translocation complex SecYEG. *J. Mol. Biol.* 352:1035–1043.

Cannon, K.S., E. Or, W.M. Clemons Jr., Y. Shibata, and T.A. Rapoport. 2005. Disulfide bridge formation between SecY and a translocating polypeptide localizes the translocation pore to the center of SecY. *J. Cell Biol.* 169:219–225.

Crowley, K.S., S. Liao, V.E. Worrell, G.D. Reinhart, and A.E. Johnson. 1994. Secretory proteins move through the endoplasmic reticulum membrane via an aqueous, gated pore. *Cell.* 78:461–471.

Erlandson, K.J., E. Or, A.R. Osborne, and T.A. Rapoport. 2008. Analysis of polypeptide movement in the SecY channel during SecA-mediated protein translocation. *J. Biol. Chem.* 283:15709–15715.

Feller, S.E., and R.W. Pastor. 1999. Constant surface tension simulations of lipid bilayers: the sensitivity of surface areas and compressibilities. *J. Chem. Phys.* 111:1281–1287.

Gullingsrud, J., and K. Schulten. 2004. Lipid bilayer pressure profiles and mechanosensitive channel gating. *Biophys. J.* 86:3496–3509.

Gumbart, J., and K. Schulten. 2006. Molecular dynamics studies of the archaeal translocon. *Biophys. J.* 90:2356–2367.

Gumbart, J., and K. Schulten. 2007. Structural determinants of lateral gate opening in the protein translocon. *Biochemistry.* 46:11147–11157.

Haider, S., B.A. Hall, and M.S.P. Sansom. 2006. Simulations of a protein translocation pore: SecY. *Biochemistry.* 45:13018–13024.

Hamman, B.D., J.C. Chen, E.E. Johnson, and A.E. Johnson. 1997. The aqueous pore through the translocon has a diameter of 40-60 Å during cotranslational protein translocation at the ER membrane. *Cell.* 89:535–544.

Hamman, B.D., L.M. Hendershot, and A.E. Johnson. 1998. BiP maintains the permeability barrier of the ER membrane by sealing the lumenal end of the translocon pore before and early in translocation. *Cell.* 92:747–758.

Harris, C.R., and T.J. Silhavy. 1999. Mapping an interface of SecY (PrlA) and SecE (PrlG) by using synthetic phenotypes and *in vivo* cross-linking. *J. Bacteriol.* 181:3438–3444.

Hashido, M., M. Ikeguchi, and A. Kidera. 2005. Comparative simulations of aquaporin family: AQP1, AQPZ, AQP0 and GlpF. *FEBS Lett.* 579:5549–5552.

Heritage, D., and W.F. Wonderlin. 2001. Translocon pores in the endoplasmic reticulum are permeable to a neutral, polar molecule. *J. Biol. Chem.* 276:22655–22662.

Higy, M., S. Gander, and M. Spiess. 2005. Probing the environment of signal-anchor sequences during topogenesis in the endoplasmic reticulum. *Biochemistry.* 44:2039–2047.

Humphrey, W., A. Dalke, and K. Schulten. 1996. VMD: visual molecular dynamics. *J. Mol. Graph.* 14:33–38.

Izrailev, S., S. Stepaniants, M. Balsera, Y. Oono, and K. Schulten. 1997. Molecular dynamics study of unbinding of the avidin-biotin complex. *Biophys. J.* 72:1568–1581.

Jensen, M.Ø., and O.G. Mouritsen. 2006. Single-channel water permeabilities of *Escherichia coli* aquaporins AqpZ and GlpF. *Biophys. J.* 90:2270–2284.

Junne, T., T. Schwede, V. Goder, and M. Spiess. 2006. The plug domain of yeast Sec61p is important for efficient protein translocation, but is not essential for cell viability. *Mol. Biol. Cell.* 17:4063–4068.

Li, W., S. Schulman, D. Boyd, K. Erlandson, J. Beckwith, and T.A. Rapoport. 2007. The plug domain of the SecY protein stabilizes the closed state of the translocation channel and maintains a membrane seal. *Mol. Cell.* 26:511–521.

MacKerell, A.D. Jr., D. Bashford, M. Bellott, R.L. Dunbrack Jr., J. Evanseck, M.J. Field, S. Fischer, J. Gao, H. Guo, S. Ha, et al. 1998. All-atom empirical potential for molecular modeling and dynamics studies of proteins. *J. Phys. Chem. B.* 102:3586–3616.

MacKerell, A.D. Jr., M. Feig, and C.L. Brooks III. 2004. Extending the treatment of backbone energetics in protein force fields: limitations of gas-phase quantum mechanics in reproducing protein conformational distributions in molecular dynamics simulations. *J. Comput. Chem.* 25:1400–1415.

Maillard, A.P., S. Lalani, F. Silva, D. Belin, and F. Duong. 2007. Deregulation of the SecYEG translocation channel upon removal of the plug domain. *J. Biol. Chem.* 282:1281–1287.

Osborne, A.R., T.A. Rapoport, and B. van den Berg. 2005. Protein translocation by the Sec61/SecY channel. *Annu. Rev. Cell Dev. Biol.* 21:529–550.

Paula, S., M. Akeson, and D. Deamer. 1999. Water transport by the bacterial channel α-hemolysin. *Biochim. Biophys. Acta.* 1418:117–126.

Phillips, J.C., R. Braun, W. Wang, J. Gumbart, E. Tajkhorshid, E. Villa, C. Chipot, R.D. Skeel, L. Kale, and K. Schulten. 2005. Scalable molecular dynamics with NAMD. *J. Comput. Chem.* 26:1781–1802.

Plath, K., W. Mothes, B.M. Wilkinson, C.J. Stirling, and T.A. Rapoport. 1998. Signal sequence recognition in posttranslational protein transport across the yeast ER membrane. *Cell.* 94:795–807.

Pohl, P. 2004. Combined transport of water and ions through membrane channels. *Biol. Chem.* 385:921–926.

Pohlschröder, M., E. Hartmann, N.J. Hand, K. Dilks, and A. Haddad. 2005. Diversity and evolution of protein translocation. *Annu. Rev. Microbiol.* 59:91–111.

Rapoport, T.A. 2007. Protein translocation across the eukaryotic endoplasmic reticulum and bacterial plasma membranes. *Nature.* 450:663–669.

Rapoport, T.A., V. Goder, S.U. Heinrich, and K.E. Matlack. 2004. Membrane-protein integration and the role of the translocation channel. *Trends Cell Biol.* 14:568–575.

Saparov, S.M., K. Erlandson, K. Cannon, J. Schaletzky, S. Schulman, T.A. Rapoport, and P. Pohl. 2007. Determining the conductance of the SecY protein translocation channel for small molecules. *Mol. Cell.* 26:501–509.

Schiebel, E., and W. Wickner. 1992. Preprotein translocation creates a halide anion permeability in the *Escherichia coli* plasma membrane. *J. Biol. Chem.* 267:7505–7510.

Simon, S., and G. Blobel. 1991. A protein-conducting channel in the endoplasmic-reticulum. *Cell.* 65:371–380.

Smith, M.A., W.M. Clemons Jr., C.J. DeMars, and A.M. Flower. 2005. Modeling the effects of *prl* mutations on the *Escherichia coli* SecY complex. *J. Bacteriol.* 187:6454–6465.

Sotomayor, M., and K. Schulten. 2004. Molecular dynamics study of gating in the mechanosensitive channel of small conductance MscS. *Biophys. J.* 87:3050–3065.

Sotomayor, M., and K. Schulten. 2007. Single-molecule experiments in vitro and in silico. *Science.* 316:1144–1148.

Tam, P.C.K., A.P. Maillard, K.K.Y. Chan, and F. Duong. 2005. Investigating the SecY plug movement at the SecYEG translocation channel. *EMBO J.* 24:3380–3388.

van den Berg, B., W.M. Clemons Jr., I. Collinson, Y. Modis, E. Hartmann, S.C. Harrison, and T.A. Rapoport. 2004. X-ray structure of a protein-conducting channel. *Nature.* 427:36–44.

Veenendaal, A.K.J., C. van der Does, and A.J.M. Driessen. 2004. The protein-conducting channel SecYEG. *Biochim. Biophys. Acta.* 1694:81–95.

White, S.H., and G. von Heijne. 2005. Transmembrane helices before, during, and after insertion. *Curr. Opin. Struct. Biol.* 15:378–386.

Wickner, W., and R. Schekman. 2005. Protein translocation across biological membranes. *Science.* 310:1452–1456.

Yang, B., and A.S. Verkman. 1997. Water and glycerol permeabilities of aquaporins 1-5 and MIP determined quantitatively by expression of epitope-tagged constructs in *Xenopus* oocytes. *J. Biol. Chem.* 272:16140–16146.

Zhu, F., E. Tajkhorshid, and K. Schulten. 2004a. Collective diffusion model for water permeation through microscopic channels. *Phys. Rev. Lett.* 93:224501.

Zhu, F., E. Tajkhorshid, and K. Schulten. 2004b. Theory and simulation of water permeation in aquaporin-1. *Biophys. J.* 86:50–57.